strongly coupled electronically and are diamagnetic.[19] Generally, Os(IV) complexes are paramagnetic, and spin-orbit coupling within the t_2^4 electronic configuration gives rise to internal t_2^4 transitions in their near-IR spectra.[16,22] The absence of such transitions in the nitrido-bridged complexes is consistent with the diamagnetism, since the diamagnetic ground state will not be affected by spin-orbit coupling. Strong coupling between the osmium centers via the p_x and p_y orbitals of the N^{3-} ligand gives rise to strong Os≡N triple bonds. The molecular orbital description of the bonding (Figure 1) is similar to that initially put forward by Griffith (for other μ-nitrido complexes)[19] and Dunitz and Orgel (for μ-oxo complexes).[23] Interactions between the ligand p_x and p_y orbitals (e_u symmetry) with the e_u combinations of the d_{xz} and d_{yz} metal ion orbitals result in strongly bonding π (e_u) and strongly antibonding π^* (e_u) combinations of orbitals. The antibonding e_g (d_{xz}, d_{yz}) combinations of the d orbitals of the metal ions remain relatively unaffected, as they do not have the correct symmetry to interact with the p orbitals of the bridging nitrido ligand. In this qualitative picture, the e_g (d_{xz}, d_{yz}) set of orbitals is the HOMO level and is filled, which gives rise to the observed diamagnetism. The strong tetragonal distortion that is induced by the strong Os≡N≡Os bonds will result in a further raising of the energy of the antibonding e_g (d_{xz}, d_{yz}) combinations, while the b_{2g} ($d_{x^2-y^2}$) and b_{1u} ($d_{x^2-y^2}$) combinations are lowered in energy. The intensities of the low-energy transitions at 21 500 and 26 000 cm^{-1} suggest that they are d-d in nature, and they have been assigned as e_g (d_{xz}, d_{yz}) → $d_{x^2-y^2}$, d_{z^2} transitions. An intense metal to ligand charge-transfer e_g (d_{xz}, d_{yz}) → e_u (π^*) transition that is z-allowed is expected, and this has been assigned to the intense transition at 40 300 cm^{-1}. The nature of the shoulder at 38 000 cm^{-1} is less certain but may be a symmetry-allowed e_g (d_{xz}, d_{yz}) → d_{z^2} transition or a δ,δ^* (d_{xy}) → $d_{x^2-y^2}$, d_{z^2} transition. A further intense charge transfer is expected between the δ (b_{1g}) combination of the d_{xy} orbitals and the e_u (π^*) orbitals. It is anticipated that this transition will be lower in intensity than the e_g → e_u transition, but it is x,y-allowed. Indeed, an intense transition is observed at 52 600 cm^{-1} for *trans,trans*-$[(Cl)(NH_3)_4OsNOs(NH_3)_4(Cl)]^{3+}$, and the rising absorption in the far-UV spectrum of $[(NH_3)_5OsNOs(NH_3)_5]^{5+}$ indicates that a similar transition occurs here. The charge-transfer transitions of the ruthenium complexes[20] are at lower energies than those of their osmium analogues. Since interactions between the ruthenium orbitals and the ligand orbitals are expected to be weaker, the difference in the energy between the e_u (π^*) and e_g orbitals would be lower. This is consistent with the assignments that have been made here.

Table II contains the tentative assignments of the transitions observed in the osmium and ruthenium nitrido complexes. More detailed analyses will require polarized spectral data and semiquantitative calculations of the energies of the electronic states.

Acknowledgment. P.A.L. gratefully acknowledges the receipt of a CSIRO Postdoctoral Fellowship and, in part, support from the Australian Research Grants Scheme. We are also grateful for support from National Science Foundation Grant No. CHE79-08633 and National Institutes of Health Grant No. GM13638-17.

(22) Piepho, S. B.; Dickinson, J. R.; Spencer, J. A.; Schatz, P. N. *Mol. Phys.* **1972**, *24*, 609-630.
(23) Dunitz, J. D.; Orgel, L. E. *J. Chem. Soc.* **1953**, 2594-2596.

Contribution from the Institut für Anorganische und Analytische Chemie, Universität Freiburg, D-7800 Freiburg, FRG, and Laboratoire de Cristallochimie, Université de Rennes, F-35042 Rennes, France

Intramolecular Conversion of an Azoalkane Ligand to Two Nitrene Ligands on a Triiron Cluster

Edward J. Wucherer,[†] Miklos Tasi,[†] Bernhard Hansert,[†] Anne K. Powell,[†] Maria-Theresa Garland,[‡] Jean-Francois Halet,[‡] Jean-Yves Saillard,[‡] and Heinrich Vahrenkamp*,[†]

Received February 16, 1989

The azoalkanes R_2N_2 (**1**; R = Et, Pr) have been reacted with $Fe(CO)_3(c\text{-}C_8H_{14})_2$ or $Fe_3(CO)_{12}$ to yield the azoalkane complexes $Fe_2(CO)_6(\mu\text{-}\eta^2\text{-}R_2N_2)$ (**2**) and $Fe_3(CO)_9(\mu_3\text{-}\eta^2\text{-}R_2N_2)$ (**3**). Thermolysis of the clusters **3** in solution has resulted in N-N cleavage without loss of CO to form the nitrene-bridged clusters $Fe_3(CO)_9(\mu_3\text{-}NR)_2$ (**4**). From the reactions of azobenzene with the iron carbonyl starting materials only products resulting from N-N cleavage have been isolated. The crystal and molecular structures of $Fe_2(CO)_6(\mu\text{-}\eta^2\text{-}Et_2N_2)$ (**2a**), $Fe_3CO)_9(\mu_3\text{-}\eta^2\text{-}Et_2N_2)$ (**3a**), and $Fe_3(CO)_9(\mu_3\text{-}NEt)_2$ (**4a**) have been determined and refined to R values of 0.076, 0.046, and 0.058, respectively. (**2a**, monoclinic, $P2_1/c$, a = 7.541 (5) Å, b = 14.609 (5) Å, c = 14.205 (4) Å, β = 106.70 (4)°, Z = 4; **3a**, monoclinic, $P2_1/n$, a = 8.860 (3) Å, b = 12.900 (2) Å, c = 16.147 (2) Å, β = 92.68 (2)°, Z = 4; **4a**, orthorhombic, *Pbca*, a = 27.214 (8) Å, b = 12.391 (8) Å, c = 11.140 (6) Å, Z = 8). With use of a mixture of the N-Et and N-Pr compounds it was ascertained that the azoalkane-nitrene cleavage is intramolecular. It is inhibited under a CO atmosphere. Kinetic analysis has shown the reaction to be approximately first order with an activation energy of ca. 35 kcal/mol. The observations can be explained by CO elimination as the first step in the rearrangement. A molecular orbital analysis with EH calculations has led to two possible pathways. One is a simple rearrangement between seven-SEP nido-type square-based-pyramidal isomers and involves a reaction intermediate or transition state in which one nitrogen atom caps an Fe_3N distorted square. The other one, which is fully consistent with the kinetic experiments, involves two intermediates with a six-SEP closo-type trigonal-bipyramidal structure; the first, resulting from CO loss and an R_2N_2 slippage, has an Fe_2N pyramidal base, while the second, due to rearrangement and N-N cleavage, has an Fe_3 pyramidal base. The final reaction step, readdition of a CO ligand, involves the opening of one Fe-Fe bond.

Introduction

Our investigations on the activation of multiply bonded organic substrates in the ligand sphere of clusters have so far been focused on C-C- and C-N-bonded systems.[1] Obvious extensions offer themselves in the form of C-O- and N-N-bonded systems. Whereas the former of these (acyl, formyl, alkoxy, alkoxycarbene) are well established in organometallic cluster chemistry, the latter (azo compounds, hydrazides) have not been used in great detail as ligands or substrates in cluster-centered reactions. In our opinion they have potential for basic cluster reactions as well as for organic reactions in the ligand sphere, due to their electron-rich

[†] Universität Freiburg.
[‡] Université de Rennes.

(1) Vahrenkamp, H. In *Organometallics in Organic Synthesis*; Werner, H., Erker, G., Eds.; Springer-Verlag: Heidelberg, FRG, 1989; p 235.

0020-1669/89/1328-3564$01.50/0

Chart I

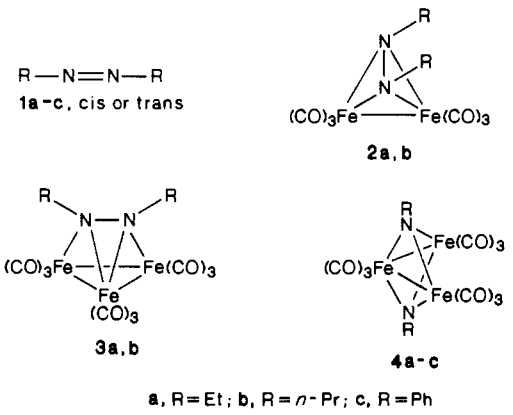

nature and their relatively weak N–N bonds.

The reported polynuclear complex chemistry of azo compounds[2] is mostly due to Kisch,[3] who investigated derivatives of polycyclic hydrocarbons. Azoalkanes have been introduced as bridging ligands in iron carbonyls.[3,4] Azoarenes were found to be cleaved or rearranged upon reactions with iron, ruthenium, and osmium carbonyls.[5] Complexes containing azoalkane ligands were also obtained from such sources as organic azides[6] or nitro compounds.[7] So far the follow-up chemistry of these systems has been limited,[3] and of the Fe_2 and Fe_3 derivatives of the simplest RN=NR ligands (i.e. R = Me, Et, Pr, Ph), only $Fe_2(CO)_6(\mu\text{-}Pr_2N_2)$ was analytically characterized,[7a] while a crystal structure determination was published for $Fe_2(CO)_6(\mu\text{-}Me_2N_2)$.[8]

We have now started to investigate the basic and derivative chemistry of polynuclear metal carbonyl complexes of the above-mentioned simple azo compounds. This paper describes the syntheses and interconversions of the products **2**, **3**, and **4** obtained from iron carbonyls and the ligands **1** (Chart I). Short communications of this work[9] and of some follow-up chemistry[10] have appeared. While this work was in progress, Bruce[11] and Gladfelter[12] reported related results on the cleavage of the N=N bonds of azoarenes upon reactions with ruthenium clusters.

Experimental Section

General Considerations. Reagent grade solvents were distilled from sodium and were stored under nitrogen. $Fe(CO)_5$ was obtained as a gift from BASF and was used without further purification. Azoethane and azopropane were prepared by the literature methods.[13]

All reactions and chromatographic separations (0.05–0.2-mm silica gel, S. T. Baker) were performed under a nitrogen atmosphere. TLC separations were carried out in air with use of plates (0.25-mm Kieselgel F_{254}) purchased from E. Merck. UV irradiation experiments were carried out in a circulating photoreactor with light from an immersion 150-W mercury lamp filtered through glass. IR spectra were recorded on a Perkin-Elmer 782 machine, NMR spectra were run on Varian EM 360 and Bruker AC-250 machines, and mass spectra were obtained on a Finnigan 4000 machine. The fraction of petroleum ether boiling between 60 and 70 °C was used.

Reactions of $Fe(CO)_3(C_8H_{14})_2$ with Azo Compounds. a. *trans*-Azoethane. To 110 mL of a petroleum ether solution of $Fe(CO)_3(C_8H_{14})_2$ (8.21 mmol) prepared according to the published procedure[14] was added 360 mg of *trans*-azoethane (4.17 mmol) at −30 °C, and the reaction solution was warmed to ambient temperature over 24 h. During this time the color of the solution changed from pale yellow to dark orange. The solution was filtered and concentrated, under vacuum, and 810 mg (54%) of **2a** was obtained as orange crystals at −30 °C and characterized by EI-MS. The mother liquor was further concentrated and chromatographed on a silica gel column. Petroleum ether eluted an additional 120 mg of **2a** (total yield 61%); petroleum ether/CH_2Cl_2 (8/2) eluted 25 mg (2%) of **3a** as a green band and traces of the orange $Fe_2(CO)_6(\mu\text{-}\eta^2\text{-}EtNCONEt)$ compound.[7b] Higher yields of **3a** (up to 20%) can be obtained by performing the reaction with the molar ratio $Fe(CO)_3(C_8H_{14})_2$:N_2Et_2 = 3:1. Anal. Calcd for $C_{10}H_{10}Fe_2N_2O_6$ (**2a**): C, 32.83; H, 2.75; N, 7.66. Found: C, 32.78; H, 2.76; N, 7.38. M_r = 365.9; EI-MS (*m/e*): 366 − 28*x* (*x* = 0–6; $[M]^+ - x$ CO). Anal. Calcd for $C_{13}H_{10}Fe_3N_2O_9$ (**3a**): C, 30.87; H, 1.99; N, 5.54. Found: C, 31.27; H, 1.92; N, 5.55. M_r = 505.8. EI-MS (*m/e*): 506 − 28*x* (*x* = 0–9; $[M]^+ - x$ CO).

b. *trans*-Azopropane. The reaction of 110 mL of a petroleum ether solution of 8.21 mmol of $Fe(CO)_3(C_8H_{14})_2$ and 475 mg (4.17 mmol) of *trans*-N_2Pr_2 was carried out as described above. Chromatographic separation (silica gel column) yielded 250 mg (16%) of orange **2b**[7a] and traces of green **3b** with use of petroleum ether eluent.

c. *trans*-Azobenzene. A petroleum ether solution (110 mL) of 8.21 mmol of $Fe(CO)_3(C_8H_{14})_2$ was reacted with 759 mg (4.17 mmol) of *trans*-N_2Ph_2 as described above. The reaction solution was filtered, concentrated, and chromatographed on a silica gel column. Petroleum ether eluted traces of $Fe_3(CO)_{12}$ and also traces of **4c**[11] as a purple-red band. Petroleum ether/CH_2Cl_2 (9/1) eluted 68 mg of unreacted azobenzene and an orange band, which was identified as the *o*-semidine-ligand-containing $Fe_2(CO)_6$ complex[5b,c] (1.14 g, 65%).

Using *cis*-azobenzene[15] instead of the trans isomer had no effect on the reaction.

Reaction of $Fe_3(CO)_{12}$ with Cis Azo Compounds. a. *cis*-Azoethane. The circulating photoreactor was charged with 82 mg (0.95 mmol) of *trans*-azoethane dissolved in 200 mL of petroleum ether, and the solution was photolyzed at 20 °C to prepare "in situ" *cis*-azoethane. After 40 min 400 mg (0.79 mmol) of $Fe_3(CO)_{12}$ was added to the reaction solution in portions over 30 min, and the irradiation was continued for 2 h. The solution was then filtered, concentrated under vacuum, and chromatographed on a silica gel column with use of petroleum ether as eluent. This first yielded unreacted $Fe_3(CO)_{12}$ and then 102 mg (35%) of **2a**, and with petroleum ether/CH_2Cl_2 (8/2) 34 mg (9%) of **3a** could be separated.

b. *cis*-Azopropane. The reaction of 400 mg (0.79 mmol) of $Fe_3(CO)_{12}$ and 108 mg (0.95 mmol) of *trans*-azopropane was carried out as described above. Chromatographic separation yielded 7 mg (2%) of **2b** and 40 mg (8%) of **3b**. Anal. Calcd for $C_{15}H_{14}Fe_3N_2O_9$ (**3b**): C, 33.71; H, 2.62; N, 5.24. Found: C, 33.78; H, 2.63; N, 5.18. M_r = 533.8. EI-MS (*m/e*): 534 − 28*x* (*x* = 0–9; $[M]^+ - x$ CO).

c. *cis*-Azobenzene. Photolysis of a $Fe_3(CO)_{12}$/*cis*-N_2Ph_2[15] mixture yielded no **4c**, which however was obtained as described[11] in the thermal reaction.

Reaction of 2a with $Fe_3(CO)_{12}$. The circulating photoreactor was charged with 300 mg (0.82 mmol) of **2a** dissolved in 250 mL of absolute benzene. A Soxhlet thimble containing 1.00 g (1.98 mmol) of $Fe_3(CO)_{12}$ was partly immersed in the circulating solution in the side arm of the reaction vessel, and the reaction solution was irradiated under vacuum at 45 °C for 24 h. The Soxhlet thimble was then removed with the remaining $Fe_3(CO)_{12}$ and the irradiation continued until the solution contained no more $Fe_3(CO)_{12}$ (TLC control). The solution was filtered and evaporated to dryness, the residue was dissolved in petroleum ether, and this solution was chromatographed on silica gel. Petroleum ether eluted 67 mg of unreacted **2a**; petroleum ether/CH_2Cl_2 (8/2) eluted 265 mg (0.52 mmol) of **3a** (81% yield based on the material consumed).

Thermolysis of 3a and 3b. A 100-mg (0.20-mmol) amount of **3a** was heated in 20 mL of toluene at 120 °C for 3 h in a 100-mL flask. During

(2) *Gmelin Handbuch der Anorganischen Chemie*; Springer-Verlag: Heidelberg, FRG, 1979; Eisen-Organische Verbindungen, Vol. C1, pp 127–163.
(3) (a) Albini, A.; Kisch, H. *Top. Curr. Chem.* **1976**, *65*, 105. (b) Kisch, H.; Krüger, C.; Marcolin, H. E.; Trautwein, A. X. *Z. Naturforsch.* **1987**, *42B*, 1435 and references cited therein.
(4) (a) Bennett, R. P. *Inorg. Chem.* **1970**, *9*, 2184. (b) Herberhold, M.; Golla, W. *J. Organomet. Chem.* **1971**, *26*, C27. (c) Fischer, G.; Sedelmeier, G.; Prinzbach, H.; Knoll, K.; Wilharm, P.; Huttner, G. *J. Organomet. Chem.* **1985**, *297*, 307.
(5) (a) Bagga, M. M.; Pauson, P. L.; Preston, F. J.; Reed, R. J. *Chem. Commun.* **1965**, 543. (b) Baikie, P. E.; Mills, O. S. *Chem. Commun.* **1966**, 707. (c) Bagga, M. M.; Flannigan, W. T.; Knox, G. R.; Pauson, P. L. *J. Chem. Soc. C* **1969**, 1534. (d) Bruce, M. I.; Iqbal, M. Z.; Stone, F. G. A. *J. Organomet. Chem.* **1971**, *31*, 275. (e) Dawoodi, Z.; Mays, M. J.; Raithby, P. R. *J. Chem. Soc., Chem. Commun.* **1980**, 712.
(6) Dekker, M.; Knox, G. R. *J. Chem. Soc., Chem. Commun.* **1967**, 1243.
(7) (a) Alper, H. *Inorg. Chem.* **1972**, *11*, 976. (b) Aime, S.; Milone, L.; Rosetti, R.; Stanghellini, P. L. *Gazz. Chim. Ital.* **1975**, *105*, 617.
(8) Doedens, R. J.; Ibers, J. A. *Inorg. Chem.* **1969**, *8*, 2709.
(9) Wucherer, E. J.; Vahrenkamp. H. *Angew. Chem.* **1987**, *99*, 353; *Angew. Chem., Int. Ed. Engl.* **1987**, *26*, 355.
(10) Tasi, M.; Powell, A. K.; Vahrenkamp, H. *Angew. Chem.* **1989**, *101*, 327; *Angew. Chem., Int. Ed. Engl.* **1989**, *28*, 318.
(11) Bruce, M. I.; Humphrey, M. G.; bin Shawkataly, O.; Snow, M. R.; Tiekink, R. T. *J. Organomet. Chem.* **1986**, *315*, C51; **1987**, *336*, 199.
(12) Smieja, J. A.; Gozum, J. E.; Gladfelter, W. L. *Organometallics* **1987**, *6*, 1311.
(13) Ohme, R.; Preuschof, H.; Heyne, H. U. *Org. Synth.* **1972**, *52*, 11.
(14) Fleckner, H.; Grevels, F. W.; Hess, D. *J. Am. Chem. Soc.* **1984**, *106*, 2027.
(15) Cook, A. H. *J. Chem. Soc.* **1938**, 876.

this time the color of the solution changed from green to red. The solvent was evaporated, and the dry residue was picked up in petroleum ether and was chromatographed on a silica gel column. Petroleum ether eluted 68 mg (68%) of red **4a** and then 15 mg of unreacted **3a**. At lower temperatures the rate of the reaction is slower, and upon prolonged heating at 80 °C decomposition predominates. Anal. Calcd for $C_{13}H_{10}Fe_3N_2O_9$ (**4a**): C, 30.87; H, 1.99; N, 5.54. Found: C, 31.03; H, 2.15; N, 5.42. M_r = 505.8. EI-MS (m/e): 506 − 28x (x = 0–9; $[M]^+ - x$ CO).

Thermolysis of 50 mg (0.094 mmol) of the less stable **3b** was performed at 80 °C for 5 h. Chromatographic separations as described above yielded 21 mg (42%) of **4b**[7a] (characterized by EI-MS), 8 mg (21%) of orange **2b**, and 11 mg (22%) of unreacted **3b**.

Thermolysis of the Mixture of 3a and 3b. A 38-mg (0.075-mmol) amount of **3a** and 40 mg (0.075 mmol) of **3b** were dissolved in a 100-mL flask in 20 mL of toluene and heated at 80 °C for 12 h. The solvent was evaporated, and the residue was picked up in a minimum amount of CH_2Cl_2 and was chromatographed on silica by TLC with use of petroleum ether. This yielded the following compounds in order of elution: 2.1 mg of **4b**, 5.7 mg of **4a**, 1.2 mg of **2b**, 2.6 mg of **2a**, 2.4 mg of **3b**, and 1.4 mg of **3a**. MS and ^1H NMR measurements showed no $Fe_3(CO)_9(\mu_3\text{-NEt})(\mu_3\text{-NPr})$.

Attempted Carbonylation of 2a. a. Thermally. A 30-mg (0.081-mmol) amount of **2a** dissolved in 25 mL of petroleum ether was stirred under a CO atmosphere for 24 h. As no reaction occurred, the reaction solution was transferred into a 50-mL autoclave and was pressurized with 75 bar of CO and stirred for 13 h. IR monitoring showed no reaction; therefore, the CO pressure was increased to 180 bar while the autoclave was heated to 90 °C for 8 h. IR and TLC showed no $Fe_2(CO)_6$(EtNCONEt).

b. Photolytically. A 25-mg (0.068-mmol) amount of **2a** dissolved in 110 mL of petroleum ether was irradiated under a carbon monoxide atmosphere for 17 h while being stirred vigorosly. Workup of the reaction solution by TLC as described above yielded 12 mg of **2a** recovered and 1 mg of **3a**, and partial decomposition could be observed. No $Fe_2(CO)_6$(EtNCONEt) could be detected.

Kinetic Measurements. Recrystallized **3a** was weighed into a 100-mL two-necked flask, the flask was flushed with argon, and 20 mL of decane (Aldrich Gold Label, washed with concentrated H_2SO_4 and distilled from sodium under argon) was introduced into the flask with a volumetric pipet. A reflux condenser and mercury bubbler were placed on the top of the reaction flask, the system was flushed with argon again, and the flask was immersed in a thermostated triethylene glycol bath. IR samples were taken through a rubber septum with a syringe and were immediately injected into an argon-flushed IR cell. The disappearance of the IR band of **3a** at 2033 cm^{-1} was monitored. The speed of the reaction and the amount of decomposition were critically dependent on the size of the reaction flask, the atmosphere in it, and the concentration of **3a**. The reaction did not proceed under a CO atmosphere, at temperatures below 105 °C decomposition was faster than the **3a** → **4a** conversion, and under vacuum or under a stream of nitrogen almost all starting material decomposed slowly. The chosen setup represents the optimum conditions for the reaction, and the measurements were reproducible for a given set of conditions.

Crystallographic Analyses. Orange crystals of **2a**, dark green crystals of **3a**, and red crystals of **4a** were obtained by cooling and slow evaporation from *n*-pentane. The crystal quality was checked, and the space groups and approximate cell constants were obtained by photographic techniques. The crystals were then mounted on a Nonius CAD4 diffractometer controlled by a PDP 11 computer. Exact lattice constants were obtained from the location of 24 reflections. The data sets were obtained at room temperature with the Nonius SDP programs. In all three cases the empirical absorption correction[16] was applied. All calculations were done with the SHELX programs.[17] The structures were solved by Patterson methods and refined anisotropically, by using unit weights, ignoring reflections with $I \leq 3\sigma(I)$, and including H atoms with a fixed C–H distance and a common fixed isotropic temperature factor. Structure factors were from Cromer and Mann.[18] In all three cases the maxima in the final difference Fourier maps were less than 1 e/Å^3. Drawings were made with SCHAKAL 84.[19] Table I summarizes the crystallographic data.

Computational Procedures for MO Calculations. All the calculations have been carried out within the extended Hückel formalism[20] by using the weighted H_{ij} formula.[21] The utilized atomic parameters have been taken from the literature.[22] The geometries for **3** and **4** were taken from the X-ray data. The following bond distances (Å) were assumed for **5**: Fe–Fe = 2.53; N–N = 1.38; Fe–N = 1.90 and 1.98. The geometries of **6** and **8** were idealized from the X-ray structures of compounds of type **3** and of $Fe_3(CO)_9(\mu_3\text{-}\eta^2\text{-}C_2Ph_2)$.[23] In the other intermediates the following bond distances (Å) were assumed: Fe–Fe = 2.50; Fe–N = 1.95. In all the calculations the following distances (Å) were used: Fe–C = 1.80; C–O = 1.15; N–H = 1.02. A system of internal coordinates has been used, in which the five skeletal atoms were defined with respect to the centroid of the cage. The energy profiles of the various transits investigated were determined from hypothetical reaction coordinates based on a linear transit of the internal coordinates between the geometries of the starting and final points. It has been checked that reasonable changes in bond distances and angles for any of the considered structures do not significantly change the results. In Schemes I–VII and Chart II the black and white dots represent nitrogen atoms while the vertices labeled from 1 to 3 are iron atoms.

Table I. Crystallographic Data

	2a	3a	4a
space group	$P2_1/c$	$P2_1/n$	$Pbca$
a, Å	7.541 (5)	8.860 (3)	27.214 (8)
b, Å	14.609 (5)	12.900 (2)	12.391 (8)
c, Å	14.205 (4)	16.147 (2)	11.140 (6)
β, deg	106.70 (4)	92.68 (2)	
V, Å^3	1499.0 (3)	1843.4 (2)	3756.3 (6)
Z	4	4	8
d_{calcd}, g/cm^3	1.62	1.82	1.79
radiation		Mo Kα	
monochromator		graphite	
cryst size, mm			
a	0.68	0.25	0.71
b	0.45	0.21	0.34
c	0.20	0.18	0.28
indices measd	$\pm h,+k,+l$	$\pm h,+k,+l$	$+h,+k,+l$
max 2θ, deg	48	48	50
scan speed, deg/min	0.7–6	0.6–6	0.8–7
scan width, deg		0.80 + 0.45 tan θ	
no. of data, $I \geq 3\sigma(I)$	1933	2657	2794
no. of unique data	2356	3157	3739
no. of variables	181	245	245
final R value	0.076	0.046	0.058

Reactions

We have found that the azoalkanes **1a,b** can be converted to their diiron complexes **2a,b** and their triiron complexes **3a,b** in good yields if heating of the reagents is avoided. The two applicable reaction pathways require photochemical activation of the iron carbonyl used. One of them involves the photolytic preparation of bis(cyclooctene)iron tricarbonyl[14] at low temperatures, which is then used as the source of $Fe(CO)_3$ units. The other uses the photolytic fragmentation of $Fe_3(CO)_{12}$ in a solution of constant and low $Fe_3(CO)_{12}$ concentration.[24] Both reactions produce mixtures of the complexes **2** and **3**, with **2** dominating and the amount of **3** depending on the excess of the iron reagent. The best way to make **3** is to isolate **2** first and then to react it again with $Fe_3(CO)_{12}$ under irradiation. Due to the easy accessibility of the iron carbonyls and the azoalkanes, compounds **2** and **3** are available in good quantities for further studies now.

Our reactions, like other routes described to obtain **2**- and **3**-type compounds,[3a,5c,6,7] have produced as byproducts the complexes $Fe_2(CO)_6(\mu\text{-RNCONR})$ formally resulting from CO insertion into the N–N bonds. To test whether compounds **2** are intermediates in their formation, **2a** was reacted with CO under various conditions, such as changing the temperature and CO pressure and applying UV light. No formation of the μ-RNCONR complex could be observed. This means that the RN–CO combination occurs during a side reaction of unknown kind. It reaffirms that N=N cleavage does not occur for these systems under photolytic conditions.

(16) Walker, N.; Stuart, D. *Acta Crystallogr.* **1983**, *A39*, 159.
(17) Sheldrick, G. M. Universität Göttingen, 1986.
(18) Cromer, D. T.; Mann, L. J. *Acta Crystallogr.* **1968**, *A24*, 321.
(19) Keller, E. Universität Freiburg, 1984.
(20) Hoffmann, R. *J. Chem. Phys.* **1963**, *39*, 1397.
(21) Ammeter, J. H.; Bürgi, H. B.; Thibeault, J. C.; Hoffmann, R. *J. Am. Chem. Soc.* **1978**, *100*, 3686.
(22) Summerville, R. H.; Hoffmann, R. *J. Am. Chem. Soc.* **1976**, *98*, 7240.
(23) Blount, J. F.; Dahl, L. F.; Hoogzand, C.; Hübel, W. J. *J. Am. Chem. Soc.* **1966**, *88*, 292.
(24) Jaeger, J. T.; Vahrenkamp, H. *Organomeallics* **1988**, *7*, 1746.

We failed to make the **2** and **3** azobenzene derivatives. In our attempts to do so with the photochemical technique we could only reproduce the results obtained thermally;[5a-c,6] i.e., the only isolable products were the nitrene-capped cluster **4c** and the semidine-bridged complex $Fe_2(CO)_6(\mu\text{-}PhNC_6H_4NH)$. Obviously the N=N bonds of azoarenes are cleaved much more easily in the presence of group 8 metal carbonyls.[11,12]

The fact that the clusters **3** were now available in good quantities allowed us to test the viability of an isoelectronic analogy, namely that between the (μ_3-η^2-azoalkane)trimetal systems and the large number of corresponding μ_3-η^2-alkyne systems.[25] Of the latter, several can undergo thermally induced cleavage of the C≡C bond accompanied by CO loss with formation of the corresponding bis(alkylidyne)-bridged clusters,[26] which reaction can also be reversed.[27] On the basis of this and on the knowledge of the easy N=N scission of azoarenes (see above) it was to be expected that thermal treatment of the clusters **3** would also result in the conversion of the azoalkane ligand into two nitrene ligands.

The verification of this assumption required temperatures of about 100 °C in hydrocarbon solvents. **3a** and (more easily) **3b** were converted to **4a** and **4b** in about 2 h. For these reactions a delicate balance of temperature, substrate concentration, and reaction atmosphere had to be maintained (see Kinetic Study). For good yields of **4** there is a temperature window of about 20 °C, since decomposition prevails at lower or higher temperatures. The stoichiometry of the **3** → **4** conversion is different from that for the corresponding alkyne-cleavage reactions in that no CO is eliminated and the elemental compositions of **3** and **4** are identical. However, the kinetic study (see below) suggests that the reaction sequence involves intermediate CO elimination.

In order to provide a sounder basis for the kinetic and theoretical studies of this reaction, proof was sought for its intramolecular nature. This is important since fragmentation/recombination is such a common aspect of cluster reactivity.[28] Definite proof might be obtained by using starting materials with isotopically labeled iron atoms. Since these were not available, a crossover experiment was performed with use of a mixture of **3a** and **3b** for the thermolysis. Its result was that the nitrene units are not interchanged between the clusters; i.e., the product mixture contained **4a** and **4b** but not the mixed compound $Fe_3(CO)_9(\mu_3\text{-}NEt)(\mu_3\text{-}NPr)$. This allows the statement that NR or $(CO)_3FeNR$ fragments are not viable reaction intermediates, which can be related with some confidence with an intramolecular reaction pathway.

Since the six-electron azoalkane ligand is converted to two four-electron nitrene ligands, the formal *metallic* electron count of the triiron complex rises from 48 to 50. This means that one metal–metal bond has to be given up, as is observed. An alternative view of the **3** → **4** interconversion is provided by the polyhedron skeletal electron pair theory (PSEP),[29] which considers both molecular structures as belonging to the same nido-type category. Indeed, the two five-vertex clusters are related to the same fundamental polyhedron, i.e. a square-based pyramid or an octahedron with one vacant vertex (see the structure determinations below), in agreement with their seven skeletal electron pairs (SEP's) or their total cluster electron count of 50 (42 ($Fe_3(CO)_9$) + 4 (NEt) + 4 (NEt) = 50). One aspect of the mechanistic considerations, therefore, is the question of how the two square-based pyramids might be interchanged (see EHMO calculations below).

The identity of the products **2**, **3**, and **4** could be ascertained from their IR spectra (see Table II) since reference compounds are available.[3-7] The NMR data support the symmetrical nature of **2** and **4**, and they give evidence for the diastereotopical nature of the (N)–CH_2 groups in **3** by the splitting of their ^1H NMR signals.

Table II. Spectra of Compounds

no.	IR[a]	^1H NMR[b]
2a	2080 (w), 2033 (s), 1993 (vs), 1975 (s), 1965 (m)	3.16 (q, 4 H, J = 7.2) 1.24 (t, 6 H, J = 7.3)
2b	2078 (w), 2030 (s), 1989 (vs), 1968 (s), 1957 (w)	3.17 (m, 4 H) 1.84 (m, 4 H) 1.01 (t, 6 H, J = 7.0)
3a[c]	2079 (w), 2033 (vs), 1992 (s), 1978 (sh), 1970 (w)	4.18 (q, 2 H, J = 7.3) 3.21 (q, 2 H, J = 7.4) 1.60 (t, 6 H, J = 7.3)
3b[c]	2078 (w), 2026 (vs), 1989 (s), 1973 (sh), 1966 (w)	4.10 (m, 2 H) 3.16 (m, 2 H) 2.11 (m, 4 H) 1.11 (t, 6 H, J = 7.1)
4a	2053 (s), 2036 (s), 1999 (vs), 1970 (w), 1962 (vw)	3.47 (q, 4 H, J = 7.5) 1.37 (t, 6 H, J = 7.5)
4b	2054 (s), 2037 (s), 1998 (vs), 1975 (sh), 1970 (w)	3.41 (m, 4 H) 1.76 (m, 4 H) 0.99 (t, 6 H, J = 7.5)

[a] ν(CO) (cm^{-1}), in pentane. [b] δ (ppm) in $CDCl_3$ (TMS); J in Hz. [c] At high field and high resolution the NMR spectra of **3a** and **3b** showed additional coupling of the CH_2 groups with the N atom ($J \approx 7$ Hz).

Table III. Atomic Parameters for **2a**

atom	x	y	z	U_{eq}, Å^2
Fe1	0.1042 (3)	0.2853 (1)	0.6998 (1)	0.0343 (9)
Fe2	0.1348 (3)	0.0718 (1)	0.3000 (1)	0.0348 (9)
N1	0.288 (2)	0.3747 (8)	0.7313 (7)	0.037 (6)
N2	0.287 (1)	0.3242 (7)	0.8124 (7)	0.032 (5)
C1	0.459 (2)	0.403 (1)	0.709 (1)	0.049 (8)
H11	0.554 (2)	0.433 (1)	0.773 (1)	0.0800 (0)
H12	0.523 (2)	0.344 (1)	0.686 (1)	0.0800 (0)
C2	0.460 (2)	0.288 (1)	0.8846 (9)	0.045 (7)
H21	0.531 (2)	0.243 (1)	0.8471 (9)	0.0800 (0)
H22	0.550 (2)	0.344 (1)	0.9171 (9)	0.0800 (0)
C3	0.408 (2)	0.474 (1)	0.624 (1)	0.07 (1)
H31	0.532 (2)	0.495 (1)	0.606 (1)	0.0800 (0)
H32	0.343 (2)	0.532 (1)	0.646 (1)	0.0800 (0)
H33	0.313 (2)	0.443 (1)	0.560 (1)	0.0800 (0)
C4	0.406 (2)	0.235 (1)	0.964 (1)	0.06 (1)
H41	0.529 (2)	0.209 (1)	1.016 (1)	0.0800 (0)
H42	0.316 (2)	0.179 (1)	0.931 (1)	0.0800 (0)
H43	0.334 (2)	0.280 (1)	1.001 (1)	0.0800 (0)
C10	−0.041 (2)	0.317 (1)	0.578 (1)	0.054 (9)
O10	−0.121 (2)	0.335 (1)	0.5006 (9)	0.098 (9)
C11	−0.076 (2)	0.236 (1)	0.739 (1)	0.047 (8)
O11	−0.194 (2)	0.2056 (8)	0.767 (1)	0.075 (8)
C12	0.200 (2)	0.185 (1)	0.666 (1)	0.047 (8)
O12	0.259 (2)	0.1154 (8)	0.647 (1)	0.082 (8)
C20	−0.019 (2)	0.495 (1)	0.713 (1)	0.048 (8)
O20	−0.123 (2)	0.5395 (9)	0.650 (1)	0.081 (8)
C21	−0.005 (2)	0.411 (1)	0.879 (1)	0.049 (8)
O21	−0.102 (2)	0.396 (1)	0.9297 (9)	0.085 (9)
C22	0.275 (2)	0.515 (1)	0.874 (1)	0.046 (8)
O22	0.358 (2)	0.5740 (9)	0.9197 (9)	0.082 (8)

Table IV. Selected Distances and Angles for **2a**

	Distances (Å)		
Fe1–Fe2	2.500 (4)	Fe2–N2	1.88 (1)
Fe1–N1	1.87 (1)	N1–N2	1.37 (1)
Fe1–N2	1.87 (1)	N1–C1	1.47 (2)
Fe2–N1	1.89 (1)	N2–C2	1.51 (2)
	Angles (deg)		
Fe1–N1–Fe2	83.7 (2)	Fe2–N2–N1	68.7 (6)
Fe1–N2–Fe2	83.4 (4)	N1–Fe1–N2	43.1 (4)
Fe1–N1–N2	68.8 (6)	N1–Fe2–N2	42.7 (9)
Fe1–N2–N1	68.1 (6)	N1–N2–C2	122.9 (9)
Fe2–N1–N2	68.6 (8)	N2–N1–C1	123.6 (9)

Molecular Structures

In order to further establish the isoelectronic relation between the azoalkane- and alkyne-bridged polynuclear complexes and to

(25) Sappa, E.; Tiripicchio, A.; Braunstein, P. *Chem. Rev.* **1983**, *83*, 203.
(26) (a) Clauss, A. D.; Shapley, J. R.; Wilker, C. N.; Hoffmann, R. *Organometallics* **1984**, *3*, 619. (b) Nuel, D.; Dahan, F.; Mathieu, R. *Organometallics* **1985**, *4*, 1436.
(27) (a) Yeh, W. Y.; Shapley, J. R. *J. Organomet. Chem.* **1986**, *315*, C29. (b) Suades, J.; Dahan, F.; Mathieu, R. *Organometallics* **1988**, *7*, 47.
(28) Vahrenkamp. H. *Adv. Oranomet. Chem.* **1983**, *22*, 169.
(29) (a) Wade, K. *Adv. Inorg. Chem. Radiochem.* **1976**, *18*, 1. (b) Mingos, D. M. P. *Acc. Chem. Res.* **1984**, *17*, 311.

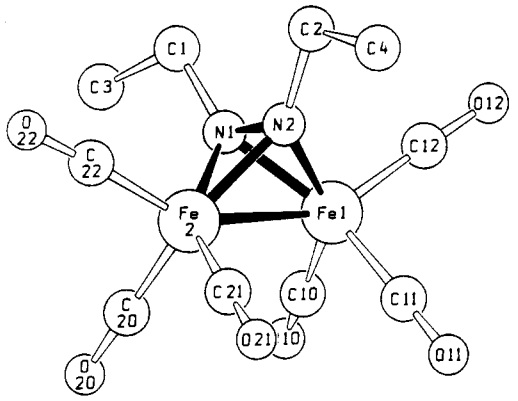

Figure 1. Molecular structure of **2a**.

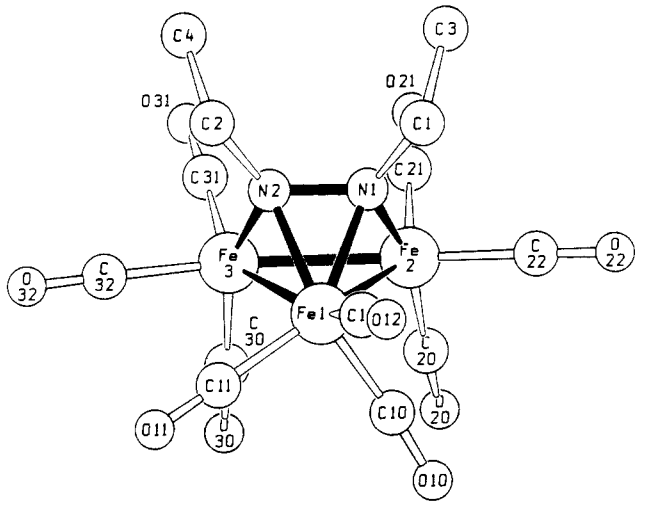

Figure 2. Molecular structure of **3a**.

fully identify the product types **2**, **3**, and **4**, the crystal and molecular structures of **2a**, **3a**, and **4a** were determined. The determinations posed no problems, and the refinements resulted in good R values.

The results for **2a** are given in Tables III and IV and in Figure 1. **2a** belongs to the large class of iron complexes with tetrahedral Fe_2E_2 cores. The simplest reference compound is $Fe_2(CO)_6(\mu\text{-}Me_2N_2)$.[8] The pertinent molecular details of both compounds are nearly identical. The iron–iron bond length of 2.50 Å is somewhat large as compared to 2.40 Å in $Fe_2(CO)_6(\mu\text{-}NH_2)_2$,[30] probably due to angle strain at the nitrogen atoms. The N–N bond (1.37 Å) is typically lengthened about 0.11 Å with respect to the value of 1.26 Å in free azoalkanes.

The isoelectronic counterpart of **2a** in the alkyne series is $Co_2(CO)_6(\mu\text{-}R_2C_2)$, of which the structures for R = t-Bu and Ph were determined.[31] The Co–Co and C–C bond lengths (2.46 and 1.34 Å, respectively) are indeed very close to the Fe–Fe and N–N bond lengths in **2a**, while the Co–C bonds (2.00 Å average) are noticeably longer than the Fe–N bonds (1.88 Å average). It is, however, difficult to assess to what extent this reflects differences in the covalent radii of C and N or differences in the bonding modes of the R_2C_2 and R_2N_2 ligands.

The structural information for **3a** is given in Tables V and VI and in Figure 2. There are no structure determinations for $Fe_3(CO)_9(\mu_3\text{-}\eta^2\text{-}E_2)$ complexes except for that of the directly related μ_3-η^2-diazanorbornene complex.[32] The bond distances in the Fe_3N_2 cores of both compounds compare favorably except for the Fe–Fe distances, which are on the average 0.04 Å shorter

Table V. Atomic Parameters for **3a**

atom	x	y	z	U_{eq}, Å^2
Fe1	0.0443 (1)	0.1241 (1)	0.3496 (1)	0.0273 (5)
Fe2	0.0783 (1)	0.2969 (1)	0.2758 (1)	0.0275 (5)
Fe3	−0.1791 (1)	0.2451 (1)	0.3296 (1)	0.0273 (5)
N1	0.1068 (6)	0.2600 (4)	0.3901 (3)	0.027 (3)
N2	−0.0329 (6)	0.2337 (4)	0.4199 (3)	0.027 (3)
C1	0.2410 (8)	0.2797 (6)	0.4474 (5)	0.040 (4)
H11	0.2296 (8)	0.2346 (6)	0.5031 (5)	0.0600 (0)
H12	0.3412 (8)	0.2555 (6)	0.4170 (5)	0.0600 (0)
C2	−0.0604 (9)	0.2286 (6)	0.5103 (4)	0.042 (4)
H21	−0.1402 (9)	0.1673 (6)	0.5210 (4)	0.0600 (0)
H22	0.0451 (9)	0.2121 (6)	0.5439 (4)	0.0600 (0)
C3	0.259 (1)	0.3934 (7)	0.4711 (6)	0.054 (5)
H31	0.358 (1)	0.4027 (7)	0.5122 (6)	0.0600 (0)
H32	0.160 (1)	0.4186 (7)	0.5021 (6)	0.0600 (0)
H33	0.272 (1)	0.4394 (7)	0.4160 (6)	0.0600 (0)
C4	−0.123 (1)	0.3298 (7)	0.5414 (5)	0.058 (6)
H41	−0.141 (1)	0.3233 (7)	0.6068 (5)	0.0600 (0)
H42	−0.229 (1)	0.3468 (7)	0.5083 (5)	0.0600 (0)
H43	−0.044 (1)	0.3915 (7)	0.5312 (5)	0.0600 (0)
C10	0.100 (1)	0.0952 (6)	0.2463 (5)	0.047 (5)
O10	0.1334 (9)	0.0658 (5)	0.1836 (4)	0.074 (5)
C11	−0.0956 (9)	0.0238 (6)	0.3526 (5)	0.042 (4)
O11	−0.1792 (7)	−0.0419 (5)	0.3569 (4)	0.065 (4)
C12	0.1865 (9)	0.0464 (6)	0.4021 (6)	0.047 (5)
O12	0.2743 (8)	−0.0058 (6)	0.4334 (6)	0.086 (5)
C20	0.0242 (9)	0.2918 (7)	0.1678 (5)	0.044 (5)
O20	−0.0053 (8)	0.2893 (6)	0.0984 (4)	0.075 (5)
C21	0.0306 (9)	0.4307 (7)	0.2819 (5)	0.045 (5)
O21	0.0050 (8)	0.5165 (5)	0.2825 (5)	0.076 (5)
C22	0.2774 (9)	0.3127 (6)	0.2545 (5)	0.042 (4)
O22	0.3988 (7)	0.3254 (6)	0.2379 (5)	0.069 (4)
C30	−0.2520 (8)	0.2189 (6)	0.2272 (5)	0.036 (4)
O30	−0.3010 (7)	0.2009 (5)	0.1620 (3)	0.054 (4)
C31	−0.2613 (9)	0.3727 (7)	0.3385 (5)	0.045 (5)
O31	−0.3164 (8)	0.4504 (5)	0.3457 (5)	0.075 (5)
C32	−0.3352 (9)	0.1792 (7)	0.3771 (5)	0.045 (5)
O32	−0.4363 (7)	0.1407 (6)	0.4035 (5)	0.075 (5)

Table VI. Selected Distances and Angles for **3a**

	Distances (Å)		
Fe1–Fe2	2.552 (1)	Fe2–N1	1.911 (5)
Fe2–Fe3	2.566 (1)	Fe3–N2	1.911 (5)
Fe1–Fe3	2.530 (1)	N1–N2	1.391 (8)
Fe1–N1	1.943 (6)	N1–C1	1.494 (9)
Fe1–N2	1.956 (5)	N2–C2	1.492 (9)
	Angles (deg)		
Fe3–Fe1–Fe2	60.7 (1)	Fe2–N1–N2	108.4 (4)
Fe1–Fe2–Fe3	59.2 (1)	Fe3–N2–N1	107.4 (4)
Fe1–Fe3–Fe2	60.1 (1)	N1–Fe1–N2	41.8 (2)
Fe1–N2–Fe3	81.7 (2)	Fe3–Fe1–N2	48.4 (2)
Fe1–N1–Fe2	82.9 (2)	Fe2–Fe1–N1	48.0 (2)
Fe1–N2–N1	68.6 (3)	C2–N2–N1	122.5 (5)
Fe1–N1–N2	69.6 (3)	C1–N1–N2	121.5 (5)

in **3a** but are in the common range for Fe_3 clusters. The N–N bond in **3a** (1.39 Å) is 0.02 Å longer than that in **2a**, in agreement with the slightly enhanced weakening due to coordination to three metal atoms. There are now two different modes of Fe–N interaction, with Fe1 being coordinated to two nitrogen atoms while Fe2 and Fe3 are each attached to one nitrogen atom. The difference in the corresponding Fe–N bond lengths (Fe1–N = 1.95 Å average, Fe2/3–N = 1.91 Å average) is, however, small. The four atoms N1, N2, Fe2, and Fe3 are nearly coplanar so that the Fe_3N_2 core can be viewed as a distorted square-based pyramid.

The alkyne series provides the cluster $FeCo_2(CO)_9(\mu_3\text{-}\eta^2\text{-}Et_2C_2)$[33] as the isoelectronic analogue for **3a**. Again the similarity of the molecular cores is striking. The average Co–Co and Co–Fe bond length is 2.52 Å, and the alkyne C–C bond is 1.37 Å long, also slightly elongated compared to that for the Co_2 alkyne complex. The alkyne in the $FeCo_2$ cluster is oriented like the

(30) Dahl, L. F.; Costello, W. R.; King, R. B. *J. Am. Chem. Soc.* **1968**, *90*, 5422.
(31) Cotton, F. A.; Jamerson, J. D.; Stults, B. R. *J. Am. Chem. Soc.* **1976**, *98*, 1774.
(32) Kisch, H.; Krüger, C.; Trautwein, A. X. *Z. Naturforsch.* **1981**, *36B*, 205.
(33) Aime, S.; Milone, L.; Osella, D.; Tiripicchio, A.; Manotti Lanfredi, A. M. *Inorg. Chem.* **1982**, *21*, 501.

Table VII. Atomic Parameters for **4a**

atom	x	y	z	U_{eq}, Å^2
Fe1	0.0917 (0)	0.1142 (1)	0.2042 (1)	0.0165 (6)
Fe2	0.1720 (0)	0.0626 (1)	0.2870 (1)	0.0168 (6)
Fe3	0.0862 (0)	−0.0815 (1)	0.2182 (1)	0.0178 (6)
N1	0.1376 (2)	0.0046 (5)	0.1497 (6)	0.016 (3)
N2	0.1076 (3)	0.0196 (5)	0.3388 (6)	0.014 (3)
C1	0.1597 (3)	−0.0071 (8)	0.0289 (8)	0.025 (5)
H11	0.1308 (3)	−0.0204 (8)	−0.0359 (8)	0.0400 (0)
H12	0.1792 (3)	0.0662 (8)	0.0067 (8)	0.0400 (0)
C2	0.0892 (4)	0.0261 (8)	0.4634 (8)	0.028 (5)
H21	0.0963 (4)	0.1064 (8)	0.4967 (8)	0.0400 (0)
H22	0.0501 (4)	0.0116 (8)	0.4621 (8)	0.0400 (0)
C3	0.1953 (4)	−0.1014 (9)	0.024 (1)	0.043 (6)
H31	0.2108 (4)	−0.1076 (9)	−0.065 (1)	0.0500 (0)
H32	0.1761 (4)	−0.1751 (9)	0.046 (1)	0.0500 (0)
H33	0.2245 (4)	−0.0885 (9)	0.089 (1)	0.0500 (0)
C4	0.1127 (5)	−0.054 (1)	0.5490 (9)	0.047 (7)
H41	0.0972 (5)	−0.044 (1)	0.6376 (9)	0.0500 (0)
H42	0.1518 (5)	−0.041 (1)	0.5525 (9)	0.0500 (0)
H43	0.1056 (5)	−0.135 (1)	0.5178 (9)	0.0500 (0)
C10	0.1177 (4)	0.2429 (9)	0.2284 (9)	0.033 (5)
O10	0.1326 (3)	0.3310 (6)	0.2411 (9)	0.053 (5)
C11	0.0324 (3)	0.1424 (7)	0.266 (1)	0.031 (5)
O11	−0.0054 (3)	0.1563 (7)	0.3096 (9)	0.057 (5)
C12	0.0722 (4)	0.1427 (9)	0.0529 (9)	0.036 (6)
O12	0.0607 (3)	0.1595 (9)	−0.0430 (7)	0.070 (6)
C20	0.2223 (3)	0.1220 (8)	0.2029 (9)	0.030 (5)
O20	0.2560 (3)	0.1586 (8)	0.1564 (8)	0.058 (5)
C21	0.1839 (3)	0.1493 (8)	0.4152 (9)	0.030 (5)
O21	0.1904 (3)	0.2059 (7)	0.4927 (8)	0.054 (5)
C22	0.2079 (4)	−0.0487 (8)	0.3366 (9)	0.029 (5)
O22	0.2297 (3)	−0.1219 (7)	0.3650 (8)	0.061 (6)
C30	0.0288 (4)	−0.1082 (8)	0.290 (1)	0.035 (6)
O30	−0.0096 (3)	−0.1229 (7)	0.3344 (9)	0.065 (6)
C31	0.0626 (4)	−0.1260 (9)	0.0742 (9)	0.035 (6)
O31	0.0489 (3)	−0.1554 (9)	−0.0147 (7)	0.066 (6)
C32	0.1147 (4)	−0.2066 (8)	0.2622 (9)	0.032 (5)
O32	0.1343 (3)	−0.2833 (6)	0.2910 (8)	0.058 (5)

Table VIII. Selected Distances and Angles for **4a**

	Distances (Å)		
Fe1–Fe2	2.457 (2)	Fe1–N1	1.944 (7)
Fe1–Fe3	2.435 (2)	Fe3–N2	1.927 (7)
Fe2···Fe3	3.037 (2)	Fe3–N1	1.918 (7)
Fe2–N2	1.920 (7)	N1···N2	2.27 (1)
Fe2–N1	1.932 (7)	N1–C1	1.48 (1)
Fe1–N2	1.952 (7)	N2–C2	1.48 (1)
	Angles (deg)		
Fe2–Fe1–Fe3	76.7 (1)	Fe1–N2–Fe3	77.8 (2)
Fe1–Fe2–Fe3	51.3 (1)	Fe3–N1–C1	127.1 (5)
Fe1–Fe3–Fe2	52.0 (1)	Fe1–N1–C1	127.9 (5)
Fe2–N1–Fe1	78.7 (3)	Fe2–N2–C2	125.2 (6)
Fe2–N1–Fe3	104.2 (3)	Fe1–N2–C2	127.8 (6)
Fe2–N2–Fe1	78.8 (2)	Fe2–N1–C1	124.0 (5)
Fe2–N2–Fe3	104.3 (3)	Fe3–N2–C2	126.0 (6)
Fe1–N1–Fe3	78.2 (3)		

azoalkane in the Fe_3 cluster, and the metal–carbon bond lengths for the π-bonding interaction (2.04 Å average) are also longer than those for the σ-bonding interactions (1.96 Å average). The complexes **2a** and **3a** thus give convincing examples of the concept of isolobal relationships.

The data for **4a** are contained in Tables VII and VIII and in Figure 3. **4a** is the third member of a series of structurally characterized compounds $Fe_3(CO)_9(\mu_3\text{-}NR)_2$,[34] the other two having R = Me[34a] and Ph.[34b] Especially, the NMe compound and **4a** can almost be superimposed. Noteworthy are the very

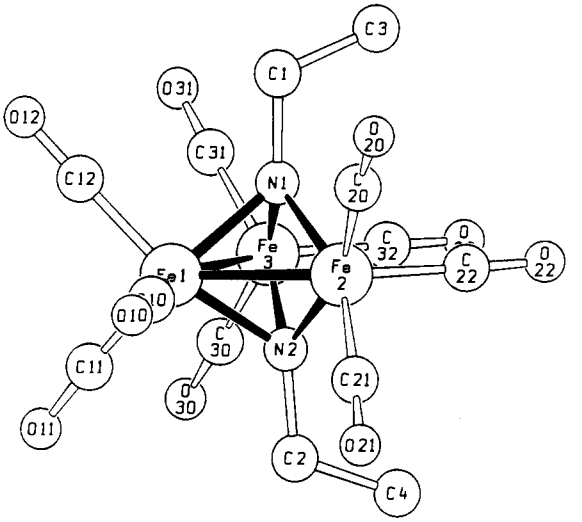

Figure 3. Molecular structure of **4a**.

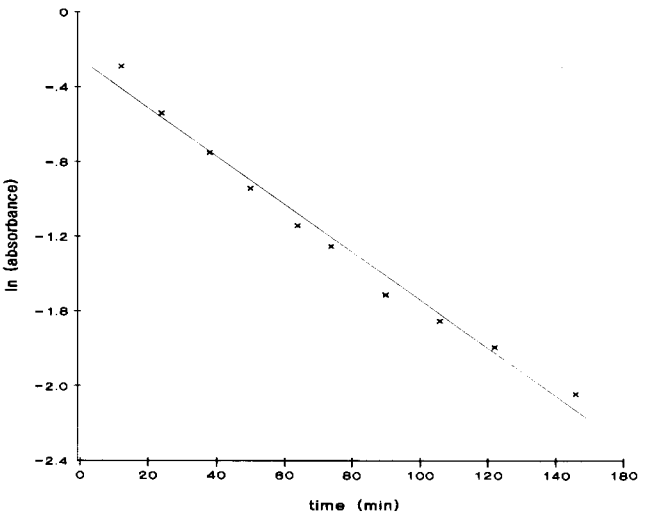

Figure 4. Kinetic run with 51.2 mg of **3a** in 20 mL of decane at 120.0 °C.

short nonbonding N–N distance of 2.27 Å and the near-planarity of the Fe2–N1–Fe3–N2 ring, which actually allows us to call **4a** a nido-type square-based-pyramidal molecule, in agreement with its seven-SEP count. The Fe–N bond lengths in **4a** are between those in **2a** and **3a**. Those involving the unique iron atom Fe1 are slightly longer than the others, but not enough to draw conclusions with respect to the bonding situation.

There is no isoelectronic analogue for **4a** in the carbon series since μ_3-alkylidyne ligands bridging open metal triangles have not yet been observed. There exists, however, a large array of $Fe_3(CO)_9(\mu_3\text{-}E)_2$ structures with four-electron ligands E from the fifth and sixth main groups.[35] All these compounds contain the open metal triangle with iron–iron bond lengths depending on the bridging ligand E. For the bonding discussion (see below) it is noteworthy that the isoelectronic cobalt clusters $Cp_3Co_3(\mu_3\text{-}E)_2$ at room temperature adopt a structure with three metal–metal interactions of equal distance, i.e. fractional bond order.[36]

Kinetic Study

The azoalkane–nitrene cleavage **3** → **4** was worth the effort of a kinetic study, which was performed with **3a** in decane. Its main objective was to find support for the intramolecular nature of the process. This could be achieved insofar as the disappearance of **3a** could best be fitted with a first-order rate law. A precise

(34) (a) Doedens, R. J. *Inorg. Chem.* **1969**, *8*, 571. (b) Clegg, W.; Sheldrick, G. M.; Stalke, D.; Bhaduri, S.; Khuaja, H. K. *Acta Crystallogr.* **1984**, *C40*, 2045. (c) For related compounds see, for example: Clegg, W.; Sheldrick, G. M.; Stalke, D.; Bhaduri, S.; Gopalkrishnan, K. S. *Acta Crystallogr.* **1984**, *C40*, 927. Williams, G. D.; Whittle, R. R.; Geoffroy, G. L.; Rheingold, A. L. *J. Am. Chem.* **1987**, *109*, 3936. Bockman, T. M.; Kochi, J. K. *J. Am. Chem. Soc.* **1987**, *109*, 7725. Bockman, T. M.; Wang, Y.; Kochi, J. K. *New J. Chem.* **1988**, *12*, 387.

(35) Cf.: Bruce, M. I. In *Comprehensive Organometallic Chemistry*; Wilkinson, G., Stone, F. G. A., Abel, E. W., Eds.; Pergamon Press: Oxford, 1982; Vol. 9, p 1209.

(36) Wakatsuki, Y. W.; Okada, T.; Yamazki, H.; Cheng. G. *Inorg. Chem.* **1988**, *27*, 2958 and references cited therein.

Scheme I

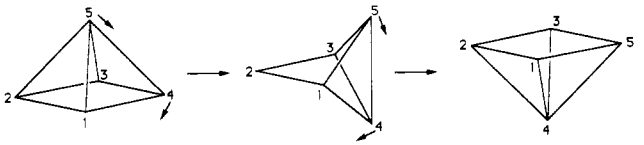

evaluation, however, was hampered by several factors.

One of these is that the reaction proceeds efficiently only in a narrow temperature window. Below 100 °C it is slower than competing decomposition reactions, while above 120 °C total decomposition sets in. Furthermore, the CO concentration in the reaction atmosphere plays a decisive role. The reaction is completely inhibited under pure CO, whereas in a nitrogen flow or under vacuum decomposition again prevails. As a result the gas volume above the reaction solution, i.e. the size of the flask, and the reagent concentration had to be optimized.

The obvious explanation for these observations is the elimination of CO at some point during the rearrangement, which has to be captured again in the end since the rearrangement proceeds without change of elemental composition. Intermediate CO elimination would also explain the detailed appearance of the kinetic plots, of which Figure 4 gives an example. The apparent first-order rate constants are always higher in the beginning than toward the end of the reaction, when the concentration of free CO rises due to the ongoing decomposition. They get smaller with an increasing initial concentration of **3a** due to the higher amount of CO liberated. They depend critically on the purity of the reagent and the solvent due to impurity-catalyzed decomposition, which liberates CO.

With these limitations in mind the kinetic data are interpretable. When solutions with 30 ± 2 mg of **3a** in 20 mL of decane were used and the observations of a 2-h period were fitted, the obtained values of the apparent first-order rate constant k were 0.0148 (15) min^{-1} at 120 °C, 0.0079 (12) min^{-1} at 115 °C, and 0.0045 (9) min^{-1} at 110 °C. From these the activation energy is calculated as $\Delta E^{\ddagger} = 36 \pm 6$ kcal/mol. With use of the initial rates, higher apparent rate constants are obtained (0.0181, 0.0126, 0.062), from which the activation energy is calculated as 33 ± 5 kcal/mol. This value is within the range of activation energies for CO displacement in polynuclear metal carbonyls,[37] although at the high end.

From the accumulated evidence one can therefore state with the necessary reservation that the **3** → **4** rearrangement is an intramolecular process which involves intermediate elimination of CO. One is therefore tempted to speculate that the loss of one CO ligand leads to the shift of the azoalkane ligand to a position orthogonally above one iron–iron bond, as is observed for the formally unsaturated clusters $Fe_3(CO)_9(\mu_3\text{-}R_2C_2)$,[25] which have the trigonal-bipyramidal Fe_3C_2 framework associated with the closo six-SEP electronic configuration. In the resulting $Fe_3(CO)_8(R_2N_2)$ intermediate the R_2N_2 ligand would be in a position from which one NR unit could flip to the other side of the Fe_3 triangle. The intermediate $Fe_3(CO)_8(\mu_3\text{-}NR)_2$ thus formed would then pick up CO to give the product **4**. This proposed mechanism is in contrast with that suggested for the conversion of $Cp_3Rh_3(CO)(\mu_3\text{-}\eta^2\text{-}R_2C_2)$ to $Cp_3Rh_3(\mu_3\text{-}CR)_2$ according to an EHMO study[26a] where the CO ligand is liberated only after the alkyne scission.

MO Calculations

In order to shed light on the details of the mechanism of rearrangement possible pathways of the **3** → **4** interconversion were analyzed in terms of molecular orbitals, by means of extended Hückel calculations. The models used for **3** and **4** in the calculations were $Fe_3(CO)_9(\mu_3\text{-}\eta^2\text{-}N_2H_2)$ and $Fe_3(CO)_9(\mu_3\text{-}NH)_2$, respectively, and will be called simply **3** and **4** in the following. Details on the calculations are given in the Experimental Section.

(37) Poë, A. J. In *Metal Clusters*; Moskovits, M., Ed.; Wiley: New York, 1986; Chapter 4.

Scheme II

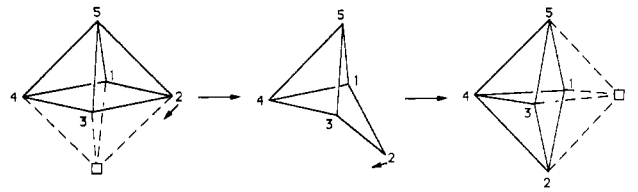

Scheme III

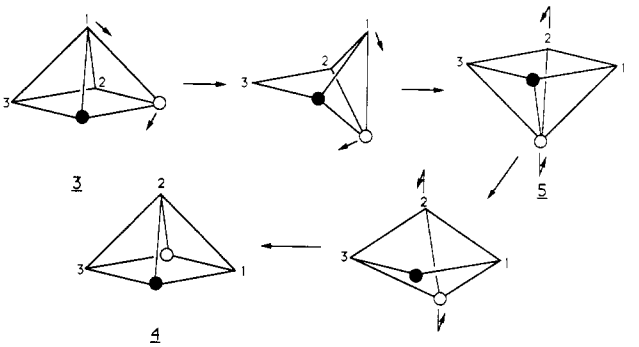

Scheme IV

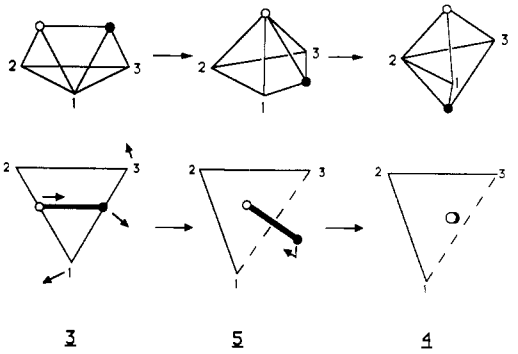

a. Interconversion Pathway without CO Exchange. The isolobal analogy makes the five-vertex seven-SEP nido-type clusters **3** and **4** equivalent to the square-based-pyramidal $C_5H_5^+$ compound. The polytopal rearrangements of this simplest cluster have been theoretically studied in detail by Stohrer and Hoffmann.[38] Their results are summarized in Scheme I. The isomerization process can be seen as a concerted mechanism, involving the breaking of a skeletal "bond" and the formation of another equivalent new bond. The transition state has a C_s symmetry in which seven skeletal bonds are preserved.

This polytopal rearrangement is rigorously equivalent to the mechanism of vertex migration on the fundamental deltahedron of a nido cluster (in our case an octahedron) proposed by McGlinchey and co-workers[39] to account for the fluxional behavior of organometallic clusters. This mechanism, shown in Scheme II, reveals that the reaction is possible because of the presence of a vacant vertex on the fundamental polyhedron of a nido cluster, which allows a facile interconversion between the isomers.

It has been shown that this kind of polytopal rearrangement can be used to account for the process of acetylene "rotation" observed in the seven-SEP nido-type $L_nM_3(\mu_3\text{-}\eta^2\text{-}C_2R_2)$ clusters[40] (species strongly related to **3**) and is in fact equivalent to the "windshield wiper" motion of the alkyne moiety above the metallic triangle proposed by Schilling and Hoffmann, on the basis of

(38) Stohrer, W. D.; Hoffmann, R. *J. Am. Chem. Soc.* **1972**, *94*, 1661.
(39) (a) Jaouen, G.; Marinetti, A.; Saillard, J.-Y.; Sayer, B. G.; McGlinchey, M. J. *Organometallics* **1982**, *1*, 225. (b) McGlinchey, M. J.; Mlekuz, M.; Bougeard, P.; Sayer, B. G.; Marinetti, A.; Saillard, J.-Y.; Jaouen, G. *Can. J. Chem.* **1983**, *61*, 1319.
(40) Mlekuz, M.; Bougeard, P.; Sayer, B. G.; Peng, S.; McGlinchey, M. J.; Marinetti, A.; Saillard, J.-Y.; Ben Naceur, J.; Mentzen, B.; Jaouen, G. *Organometallics* **1982**, *4*, 1123. See also: Gimarc, B. M.; Ott, J. J. *Inorg. Chem.* **1986**, *25*, 83.

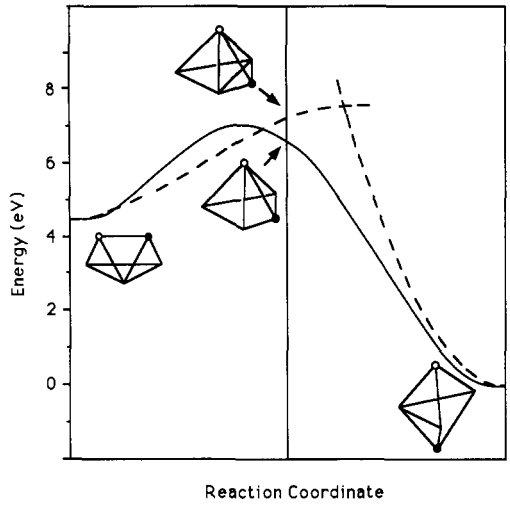

Figure 5. Energy profile of the **3** → **4** reaction assuming either **5** (solid line) or **6** (dashed line) as the intermediate structure.

extended Hückel calculations.[41] We have also investigated this process on our model **3** and calculated an energy barrier of 0.9 eV for the azoalkane rotation process, in reasonable agreement with the theoretical and experimental values found for the related acetylenic clusters.

The first pathway we explore is based on the polytopal rearrangement of Scheme I and is shown in Scheme III. It involves the intermediate **5**, which is, in terms of the PSEP theory,[29] an acceptable isomer of **3** and **4**. An alternative representation of the same two-step mechanism is shown in Scheme IV, which shows the five cluster atoms projected over the metallic triangle and the corresponding perspective view. From this representation one can see easily that the **3** → **5** interconversion consists of the opening of the Fe(1)–Fe(3) bond concerted with a sliding motion of the azoalkane moiety, which also establishes a Fe(3)–N interaction. This sliding is the composition of a translation and a rotation that turns by 30° the projection of the N–N vector over the iron triangle and brings the black nitrogen atom down to the trimetallic plane. The **5** → **4** interconversion consists of a swinging motion of the black nitrogen to the opposite side of the metallic plane to occupy a μ_3 position symmetrical to the one of the other N atom.

Our calculations on **3** and **4** are based on idealized experimental geometries (see Experimental Section). Both complexes exhibit a large HOMO–LUMO gap, 1.92 and 1.98 eV, respectively, consistent with their seven-SEP count. The MO diagram of **3** is very similar to the ones calculated for related nido-type seven-SEP $L_nM_3(\mu_3\text{-}\eta^2\text{-}C_2R_2)$ complexes.[41b,42] The isomer **4** is found more stable than **3** by ~4 eV. This is in agreement with the fact that the **4** → **3** interconversion is not experimentally observed and with the fact that the bis(nitrene) trimetallic clusters are far more common than their azoalkane isomers. Compound **5**, for which a geometry was assumed (see Experimental Section), was found less stable than **3** by 1.92 eV. However, there is no a priori reason to conclude that **5** is unstable, since its HOMO–LUMO gap of 0.77 eV appears sufficiently large to provide the molecule with a reasonable Jahn–Teller stability. It should be also noted that pentavalent nitrogen has already been observed in stable organometallic cluster compounds.[43]

The energy profiles of the **3** → **5** and **5** → **4** transits, evaluated for a hypothetical reaction coordinate, are shown in Figure 5 (solid line). Both transits are symmetry allowed (no HOMO–LUMO level crossing). From these energy profiles one can see that **5** is not a reaction intermediate but a point close to the transition state. However, considering the level of approximation of our calculations, it is not possible to conclude that **5** is better described as a transition state rather than a high-energy reaction intermediate. The energy barrier for the overall **3** → **4** transit is ~2.4 eV, a value in reasonable agreement with the experimental activation energies (vide supra).

Scheme V

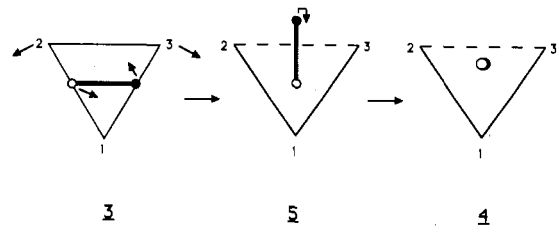

Scheme VI

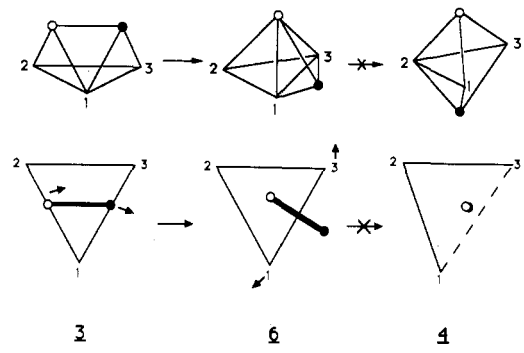

We have also explored a transit similar to the one depicted in Scheme IV but in which the N–N vector starts to open at the beginning of the reaction, at the same time as the Fe(1)–Fe(3) bond. This pathway was found disfavored because of the loss of bonding interactions near the transition state.

Another possibility for the **3** → **5** interconversion is the opening of the Fe(2)–Fe(3) bond concerted with a displacement of the N–N vector that, in projection, consists essentially of a 90° rotation (Scheme V). Our calculations found this transit less favored than the **3** → **5** least-motion pathway described above. In particular, serious steric problems occur when the projections of the Fe(2)–Fe(3) and N–N vectors start to cross. In their theoretical investigation of the related reaction of alkyne scission on a trimetallic framework Clauss et al.[26a] proposed that the first stage of the reaction is a similar "90° rotation" of the C–C bond, but *without* the opening of the Fe(2)–Fe(3) bond, leading to a closo intermediate, an isostructural rotational isomer of the cluster **6** shown in the center of Scheme VI. We found this **3** → **6** non-least-motion transit highly disfavored for two reasons: (i) Again, steric hindrances occur when the Fe(2)–Fe(3) and N–N projections start to cross. In order to avoid them, the N_2H_2 ligand has to stand high above the metallic triangle in the transition state, causing substantial loss of bonding. These steric problems are avoided in the **3** → **6** least-motion pathway, which consists of a sliding of the N–N vector so that it becomes perpendicular to Fe(1)–Fe(3) and *not* to Fe(2)–Fe(3) (first step of Scheme VI). (ii) The closo structure of **6** is stable for a six-SEP count and highly disfavorable for the seven-SEP count of $Fe_3(CO)_9(N_2R_2)$. The electronic structure of this type of M_3E_2 cluster[42] is well-known: a large HOMO–LUMO gap is observed for six SEP's (1.45 eV in the case of **6**) and a small HOMO–LUMO gap for seven SEP's (0.45 eV for **6**) associated with a strong M–E antibonding character of the HOMO, rendering **6** less stable than **3** by 2.66 eV. These findings are consistent with the calculations of Stohrer and Hoffmann on the skeletal rearrangement of $C_5H_5^+$, who found the closo structure to be the highest point of their potential energy surface[38] and consequently not to be situated on the interconversion

(41) (a) Schilling, B. E. R.; Hoffmann, R. *Acta Chem. Scand.* **1979**, *B33*, 231. (b) Schilling, B. E. R.; Hoffmann, R. *J. Am. Chem. Soc.* **1979**, *101*, 3456.

(42) (a) Granozzi, G.; Tondello, E.; Casarin, M.; Aime, S.; Osella, D. *Organometallics* **1983**, *2*, 430. (b) Halet, J.-F.; Saillard, J.-Y.; Lissillour, R.; McGlinchey, M. J.; Jaouen, G. *Inorg. Chem.* **1985**, *24*, 218. (c) Busetti, V.; Granozzi, G.; Aime, S.; Gobetto, R.; Osella, D. *Organometallics* **1984**, *3*, 1510. (d) Aime, S.; Bertoncello, R.; Busetti, V.; Gobetto, R.; Granozzi, G.; Osella, D. *Inorg. Chem.* **1986**, *25*, 4004.

(43) Gervasio, G.; Rossetti, R.; Stanghellini, P. L. *J. Chem. Soc., Chem. Commun.* **1977**, *387*.

Chart II

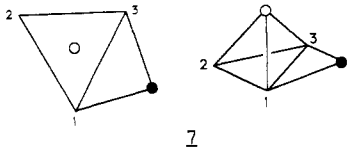

7

Scheme VII

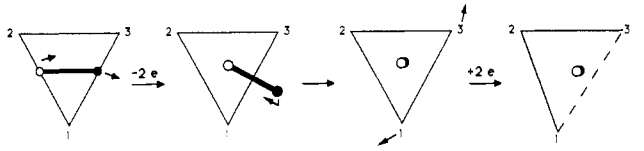

3 8 9 4

pathway of Scheme I. A simple way of stabilizing **6** is to open one of its bonds; this condition is satisfied in **5**, which is more stable than **6** by 0.74 eV. In fact, we think this energy difference is somewhat underestimated in our calculations because the molecular structure of **6** we used is probably too approximate, owing to the lack of experimental structural information for this kind of molecule.

The **6** → **4** least-motion pathway of Scheme VI, i.e. the opening of the Fe(1)–Fe(3) bond concerted with a swinging motion of the black N atom over the edge, is symmetry forbidden: there is a HOMO–LUMO level crossing between an a′ orbital of predominant metallic character that becomes Fe–N antibonding and an a″ Fe(1)–Fe(3) antibonding orbital that becomes nonbonding. The overall energy profile corresponding to the two-step **3** → **6** → **4** least-motion pathway is represented in Figure 5 (dashed line). It is clear that this mechanism is disfavored on the basis of both energy and symmetry considerations.

Another way of stabilizing the seven-SEP species **6** is to open its N–N bond as in Chart II, forming **7**, which satisfies the EAN rule and then could be a "good" reaction intermediate. Indeed, **7** was found more stable than **3** by 1.54 eV, with a large HOMO–LUMO gap (1.48 eV). However, the **7** → **4** rearrangement is symmetry forbidden for the same reason as for the **6** → **4** process. Obviously, if there is no CO exchange with the medium, the Fe–Fe bond must open before the N–N bond and then the most probable intermediate structure is **5**.

b. Interconversion Pathway Involving CO Exchange. From a theoretical point of view, the loss or gain of a two-electron ligand is formally equivalent to a decrease or an increase of two units in the cluster total electron count. Therefore, we have chosen to model the CO-exchange reactions by replacing the variation in the number of CO ligands by a change of ±2 in the electric charge of the molecule. Indeed, it is beyond the capabilities of the method we use to model all the possible ligand positions (terminal, bridging, semibridging, ...) of an eight-carbonyl Fe_3N_2 cluster during the various steps of the mechanism.

The least-motion pathway we explored is the one suggested on the basis of the kinetic experiments (vide supra). This three-step mechanism is shown schematically in Scheme VII. The first step, which corresponds to the loss of a CO ligand, leads to the product **8**, which is thermodynamically stable and isostructural and isoelectronic with the well-known $Fe_3(CO)_9(\mu_3\text{-}\eta^2\text{-}C_2Ph_2)$ complex[23] (note that **8** has the same closo structure as **6** but with a six-SEP count, in agreement with the PSEP rules). The energetic balance of the **3** → **8** reaction, assuming the two electrons lost by the cluster are going into a carbonyl σ nonbonding orbital, was found favorable. Because of the simplification we made, an evaluation of the energy barrier of this reaction was not possible but is expected to be low since the structural rearrangement is soft.

The second step is a closo → closo structural rearrangement without change in the cluster electron count (both six-SEP **8** and **9** have a trigonal-bipyramidal skeleton). This reaction can be described as a rocking motion of the black nitrogen around the Fe(1)–Fe(3) edge, so that it reaches the other side of the metal triangle (see Scheme VII). The energy profile of this rearrangement is plotted in Figure 6. In order to preserve reasonable bond distances all along the hypothetical reaction coordinate, the process was subdivided into two steps, the assumed midpoint of the reaction coordinate corresponding to the black nitrogen situated in the metallic plane (a structure identical with **7**, but with two electrons less). The reaction is symmetry allowed with a very low evaluated energy barrier (~0.14 eV), and again the reaction is thermodynamically favored. The presence of a shallow minimum on the energy curve is probably not very significant at the level of accuracy of the method.

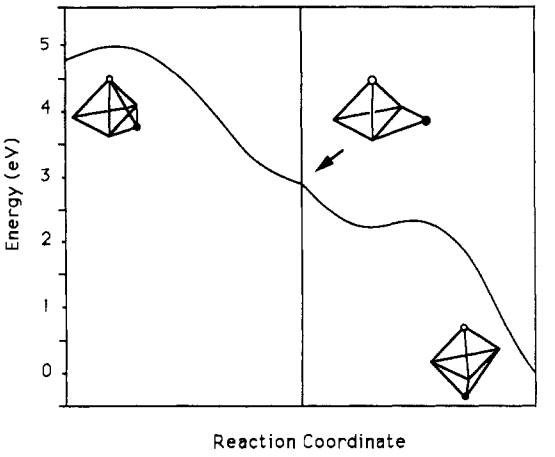

Figure 6. Energy profile of the **8** → **9** reaction assuming that the midpoint of the transit is an edge-bridged Fe_3N tetrahedron.

The last step of this process is the opening of a Fe–Fe bond while the total electron count rises by 2. Here again the structural rearrangement is soft and the activation energy is expected to be low. The evaluated energy balance of the reaction, assuming the two gained electrons come from a carbonyl lone pair, is this time positive.

c. Conclusion. It appears from this MO study that the two most probable mechanisms of rearrangement satisfy the two following conditions: (i) avoiding intermediate structures that are suited for a smaller electron count, i.e. never occupying antibonding orbitals; (ii) the first condition being necessarily satisfied, keeping the highest possible connectivity all along the reaction path.[44]

Because extended Hückel calculations yield results only at a qualitative level and because of the simplifications we maade, it is not possible to predict which one of the two mechanisms we propose is the most likely to occur. Although it was not possible to evaluate totally its energy profile, Scheme VII is the one we favor for being the real one, since our computional results are consistent with an easy pathway and are in agreement with the kinetic experiments.

Acknowledgment. This work was supported by the Fonds der Chemischen Industrie and by the Rechenzentrum der Universität Freiburg. E.J.W. thanks the Deutscher Akademischer Austauschdienst, M.T. thanks the Stiftung Volkswagenwerk, and A.K.P. thanks the Landesschwerpunktsprogramm FR-NW-31 for postdoctoral appointments.

Supplementary Material Available: For all three structure determinations, listings of all positional and anisotropic thermal parameters and all distances and angles (36 pages); listings of F_o/F_c (33 pages). Ordering information is given on any current masthead page.

(44) (a) Johnson, B. F. G. *J. Chem. Soc., Chem. Commun.* **1986**, 27. (b) Rodger, A.; Johnson, B. F. G. *Polyhedron* **1988**, *7*, 1107.